Modeling the Interaction Between Actin and Filamin 1 in the Cell Cytoskeleton

by

Christopher Allan Hartemink

B.S. Mechanical Engineering, Calvin College, 1996
B.S. Physics, Calvin College, 1996

Submitted to the Department of Mechanical Engineering
in partial fulfillment of the requirements for the degree of

Master of Science in Mechanical Engineering
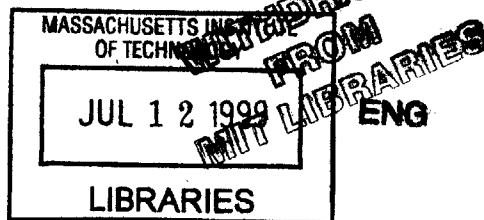
at the

MASSACHUSETTS INSTITUTE OF TECHNOLOGY

February 1999

Author...
Department of Mechanical Engineering
January 8, 1999

Certified by ....
C. Forbes Dewey, Jr.
Professor of Mechanical Engineering
Thesis Supervisor

Accepted by...
Ain A. Sonin
Departmental Graduate Officer

Modeling the Interaction Between Actin and Filamin 1 in the Cell Cytoskeleton

by

Christopher Allan Hartemink

B.S. Mechanical Engineering, Calvin College, 1996

B.S. Physics, Calvin College, 1996

Submitted to the Department of Mechanical Engineering
on January 8, 1999, in partial fulfillment of the
requirements for the degree of
Master of Science in Mechanical Engineering

Abstract

The cytoskeleton is a dense network of partially crosslinked filamentous actin that provides structure to cells. Modeling this complicated network requires understanding how its individual elements interact. Filamin 1 (known previously as ABP or ABP-280) is a large 2x280.5 kDa dimeric actin crosslinking protein found in eukaryotic cells that promotes actin filament crosslinking in orthogonal junctions. We develop a theoretical physical model for this crosslinking protein, and provide an elaborate analysis of future experiments carefully designed to the mechanical properties of filamin 1. Specifically, the new model proposed here for filamin 1 agrees with known physical data for the molecule, and explains orthogonal junctions. The model's morphology consists of two distinct regions: a stiff base region that imparts structure to the junction of two actin filaments, and flexible arm regions that attach filamin 1 to F-actin. Due to the small size of a single actin-filamin 1 junction, random Brownian forces imparted by the thermal motion of the buffer dominate the kinematics of the system. Microscopy enables determination of the deformation of filamin 1 that results from these Brownian forces. Analyzing the equation of motion for the actin-filamin 1 system enables us to determine filamin 1's resistance to deformation by measuring the angular variance of the molecule. Performing Fourier analysis on the curvature of traces of the arms enables us to quantify their flexibility. This thesis proposes the new model and carefully analyzes future experiments necessary to quantify the model.

Thesis Supervisor: C. Forbes Dewey, Jr.
Title: Professor of Mechanical Engineering

Acknowledgments

My family, more than any other thing in my life, is responsible for my success. Nowadays to even have a family is rare, but not only am I blessed to have a family, I was blessed beyond all dreams by being born into a family so marvelous.

I would also like to thank my friends at MIT for all their encouragement and support as well, specifically Jeremy Teichman, Ngon Dao, Vitaly Napadow, Mark Price, Sham Sokka, Patrick Purdon, Yuan Cheng, and Darryl Overby. It is only through their friendship that I have been able to endure my education here.

Scientifically, I owe large debts of gratitude to Jim McGrath and John Hartwig. Jim took me under his wing when I was a fledgling distraction with lots of questions, and has led me through his example. John too has been more patient and encouraging than I could ever expect from a man so prominent in his field. I give them credit for trying to teach an engineer a little biology. This document is a measure of their success.

Unable to fit exclusively in any of the above three categories is Alex: my brother, my friend, and my collaborator. As has been true for each of the past 24 years, he has been emphatic in loving me, encouraging me, and instructing me. For many years I tried unsuccessfully to follow in his footsteps; only recently did I give up when I came to the realization that he truly walks on water.

Lastly, I owe great thanks to my research advisor, C. Forbes Dewey, Jr. for taking me on, supporting me, encouraging me, challenging me, and keeping me on task, especially when my love of science sometimes got in the way of my pursuit of a degree.

Dedication

I would like to dedicate this work to three people: Two in heaven and one who makes me feel like I am already there.

- To my God. 'Tis grace has brought me safe thus far, and grace will bring me home. I am merely a tool in His hands.

- To my grandfather, Albert J. Hartemink. Despite the fact that he died thirty years before my birth, his sacrifice taught me what it means to live, and why. I can only pray that I will change the world as much in eighty years as he did in twenty five.

- To *mi tesorita*, and now fianceé, Samantha Lavery. Her love for me has been the only thing promising enough to carry me through, and so she deserves this more than I do.

Contents

List of Figures

Chapter 1

Introduction

1.1 Motivation

For many years scientists thought the cell to be an amorphous, structureless entity: a "bag of enzymes." Like a sandwich bag filled with water, the cell was thought to be primarily water, with some proteins in solution, surrounded by a soft permeable membrane. With the advent of the electron microscope, this theory came crashing down. The first electron micrographs of the cell in 1945 showed that cells are highly structured, organized units.

Immediately scientists observed a skeleton of proteins that permeated the cells, as seen in Figure 1-1. This cytoskeletal network serves many purposes. Most fundamentally, it gives the cell its mechanical structure. Like scaffolding, the network provides a framework holding everything in place, and provides rigidity and resistance to deformation from forces transmitted to and from the cell membrane. The network also provides other functions, such as regulating organelle transport and enabling cell motility.

The mechanical role is investigated here. The cytoskeletal network is composed of three polymeric proteins, the most abundant of which is actin. Actin filaments are present throughout the cytosol (the solution within the cell's membrane), providing the necessary structure. Other proteins, known as actin-binding proteins, join actin filaments together, causing the random accumulation of actin filaments to attain some order, as well as imparting added rigidity.

Exploring the interaction between actin and one of the most abundant of these crosslinking proteins, filamin 1, is the focus of this study. The overarching goal of the long-term project is to develop a model of the integrated cytoskeleton of the cell, so that cell be-
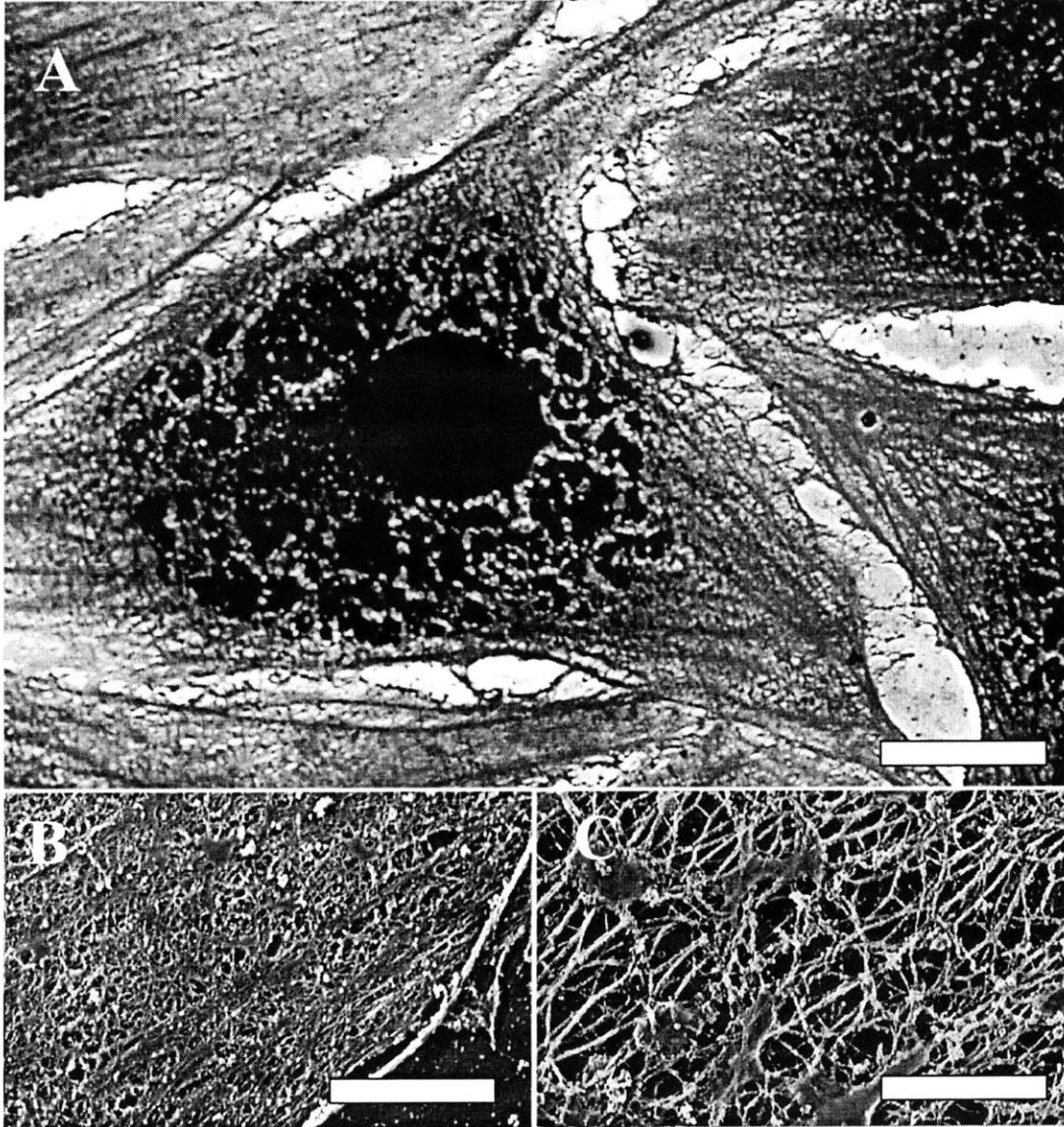
Figure 1-1: The actin cytoskeleton in endothelial cells. A. A confluent monolayer of endothelial cells with actin visible in the cortex of each cell. Bar 5 μm. B. The actin cytoskeleton of an endothelial cell shown at 5× the magnification of A. Note the density of the network that provides structure to the cell. Bar 1 μm. C. Actin filaments magnified an additional 5× higher than in B. Note the complicated three dimensional structure of the network. Bar 200 nm. Photos courtesy J. Hartwig.

havior can be predicted in response to mechanical stimuli such as shear stress. Since the network is composed predominantly of crosslinked actin filaments it is natural to start by analyzing the way actin filaments and their crosslinkers interact with each other. By first understanding the dynamics of two actin filaments joined by a single filamin 1 molecule, we can extrapolate, with necessary modifications, to begin to model the dynamics of the entire cytoskeleton.

There have been previous models of the cytoskeleton proposed, but never at this ambitious level of detail: individual protein molecules. Satcher proposed a "theoretical estimate" of the properties of the cytoskeleton [44] based on analogy to cork and bread, via Gibson and Ashby's analysis of "cellular solids" [11]. This model was highly speculative however, and glossed over necessary details. It was adequate as a first order approximation, but it is not nearly as predictive or accurate as the task undertaken here.

Ingber has proposed an artistic model of the cytoskeleton based on analogy to aesthetic architecture motifs [20], but the model is in its essence merely qualitative. Known as "tensegrity," the model proposes that the cell is essentially a geodesic sphere, with a membrane pulled tight over stress fibers which act as braces in compression. While it is known that the cell membrane is in fact in tension, this model struggles to *explain* anything about the cell. Ingber treats the cell as a statics problem, rather than as a complex dynamic living body.

This study, again, is an attempt to proceed to the *molecular* level in formulating a model of the cytoskeleton. The cytoskeleton is a large structure composed of smaller elements. By understanding these elements and how they interact, we can work outwards to understand the cytoskeleton as a whole.

1.2 The Elements of the Actin Cytoskeleton

The two proteins that we analyze are actin and filamin 1, which we introduce briefly here. In Chapter 2 we model the interaction between these two proteins, and their relevant physical and biological properties are discussed more fully there.

1.2.1 Actin

Actin is the most abundant protein in eukaryotic cells, found in concentrations on the order of 0.2-0.5 mM. It is a monomeric protein that polymerizes into long slender filaments in the presence of mono- and divalent salts and ATP. Each monomer is roughly globular in shape (hence the name *G-actin*), approximately 4 nm in diameter. When polymerized, G-actin aggregates as a polarized double-helical formation, approximately 8 nm wide and varying in length from 100 nm to 100 μm, as seen in Figure 1-2. Polarity is defined by decorating the actin filaments with myosin S1: the myosin attaches to the filaments in an arrowhead configuration, defining a barbed end and a pointed end. The cytoskeletal network is a dense mesh of this filamentous actin (*F-actin*).

F-actin is a dynamic polymer with a slow rate of turnover *in vitro* [54] that is greatly accelerated in cells [53]. Monomers are constantly being added to the barbed end and removed from the pointed end. This turnover plays a pivotal role in regulating cell motility and other dynamic properties of cells [35, 48], but does not appear important in understanding its mechanical relation to filamin 1, which is the focus of this study.

1.2.2 Filamin 1

Actin-binding proteins are a large family of proteins that, as the name implies, bind actin filaments together. These proteins can be divided into two main groups: bundling proteins and crosslinking proteins. Bundling proteins cause F-actin to align in a parallel fashion, creating large, strong reinforced struts, known as stress fibers. The other class of linking proteins, crosslinking proteins, are the focus of this study- filamin 1 in particular.

Crosslinking proteins differ from bundling proteins in that crosslinking proteins cause two actin filaments to intersect at large angles ("large" refers to angles near right angles, roughly 80° - 100°). Crosslinking proteins thus cause actin filaments to form intricate networks rather than stress fibers. The actin network is dispersed throughout the cell and is the structural element that provides support to the entire cell.

The filamins are a group of crosslinking proteins with specific properties: a dimeric structure with beta sheet repeats separating the actin-binding regions at the N-termini from the self-association site at the C-termini (see Figure 2-1). Filamin 1 is a specific crosslinking protein in this family found in nonmuscle cells and appears to be the most
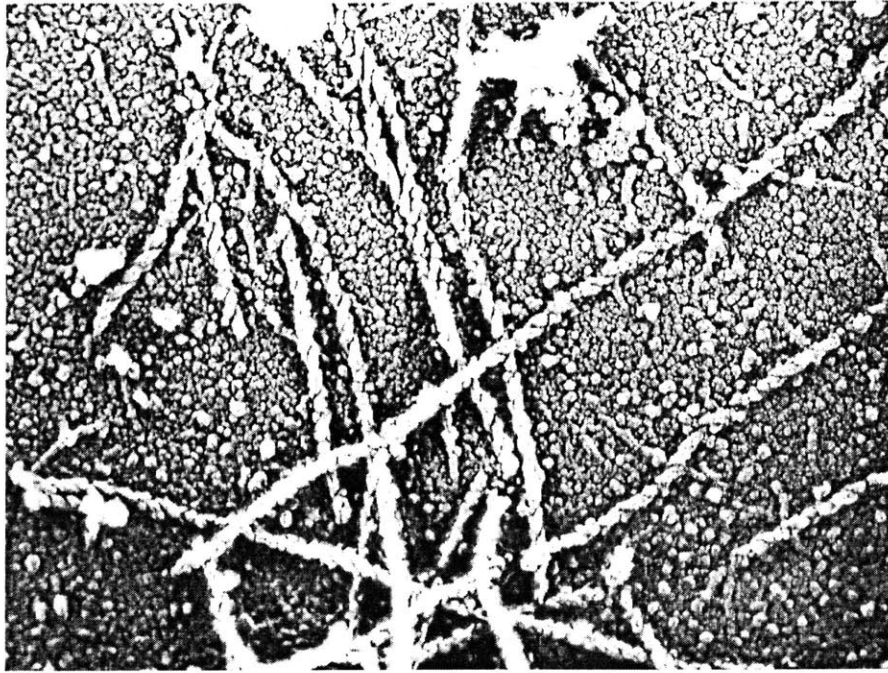
Figure 1-2: Electron micrographs of individual actin filaments. At this scale the repeat nature of F-actin is visible. These filaments are coated with myosin-S1 in order to accentuate the polarity of the filaments. Bar 100 nm. Photo courtesy J. Hartwig.

abundant and widely expressed variant in humans [29, 13]. Cell motility depends heavily on filamin 1 mediation and cells lacking filamin 1 display a remarkable loss of translational locomotion [47, 4]. Other defects of filamin-1-null cells include loss of stability as evidenced by blebbing [3, 47], impaired volume regulation [2, 47], and abnormal phagocytosis [42, 47]. These symptoms disappear when the cells are rescued by filamin 1 [4, 47]. The locus of the filamin 1 gene (FLN1) is the X chromosome, at Xq28 [13, 47]. Failure to express filamin 1 results in human periventricular heterotopia, a developmental disorder that results from the limited migration of neurons [9, 47]. Because of X inactivation, some females are able to survive with the disease but males with complete loss of filamin 1 die *in utero*.

Filamin 1 is of interest in this mechanical study because it is expressed at high concentrations (0.5 - 3.0% of total protein) and therefore as many as 40% of F-actin junctions in cells are regulated by this protein [16]. Presuming that some junctions may not be mediated by any crosslinking proteins (arising merely from steric juxtapostion), filamin 1 is considered one of the primary crosslinking proteins.

Chapter 2

Modeling

When attempting to produce a model of any kind, certain simplifications have to be made. That is what separates the model from reality. Good modeling is a cyclic process: one must make enough simplifying assumptions to make the model tractable, learn something about the system being studied, tighten the assumptions based on what has been learned, learn more, tighten the assumptions more, learn more, etc. This model is no different. This model assumes certain elements are perfectly rigid, and that others are connected perfectly, and so forth. The assumptions are supported by the data, and are necessary in order to produce a first-cut analysis of the molecular interaction. The natural place to start when modeling a system and making assumptions is examining what is already known. In Section 2.1 we review the known properties of filamin 1. Based on this knowledge of filamin 1's structure and function, in Section 2.2 we examine three possible models for filamin 1's crosslinking of actin. After discarding the two inadequate models, we reexamine the relevant physical properties of filamin 1 in Section 2.3 and propose our model in Section 2.4.

2.1   Filamin 1

2.1.1   Structure

Filamin 1 is an elongated dimeric protein, with a molecular weight of 2x280.5 kDa. Subunits are long and thin, with lengths of 80 nm and diameters of 3-5 nm. Filamin 1 dimerizes [18] with its C-terminus ends attached to each other, forming a roughly V-shaped connection, as shown in Figure 2-1.

A

N-T

Actin binding
site

Repeat 1

Repeat 24

C-T
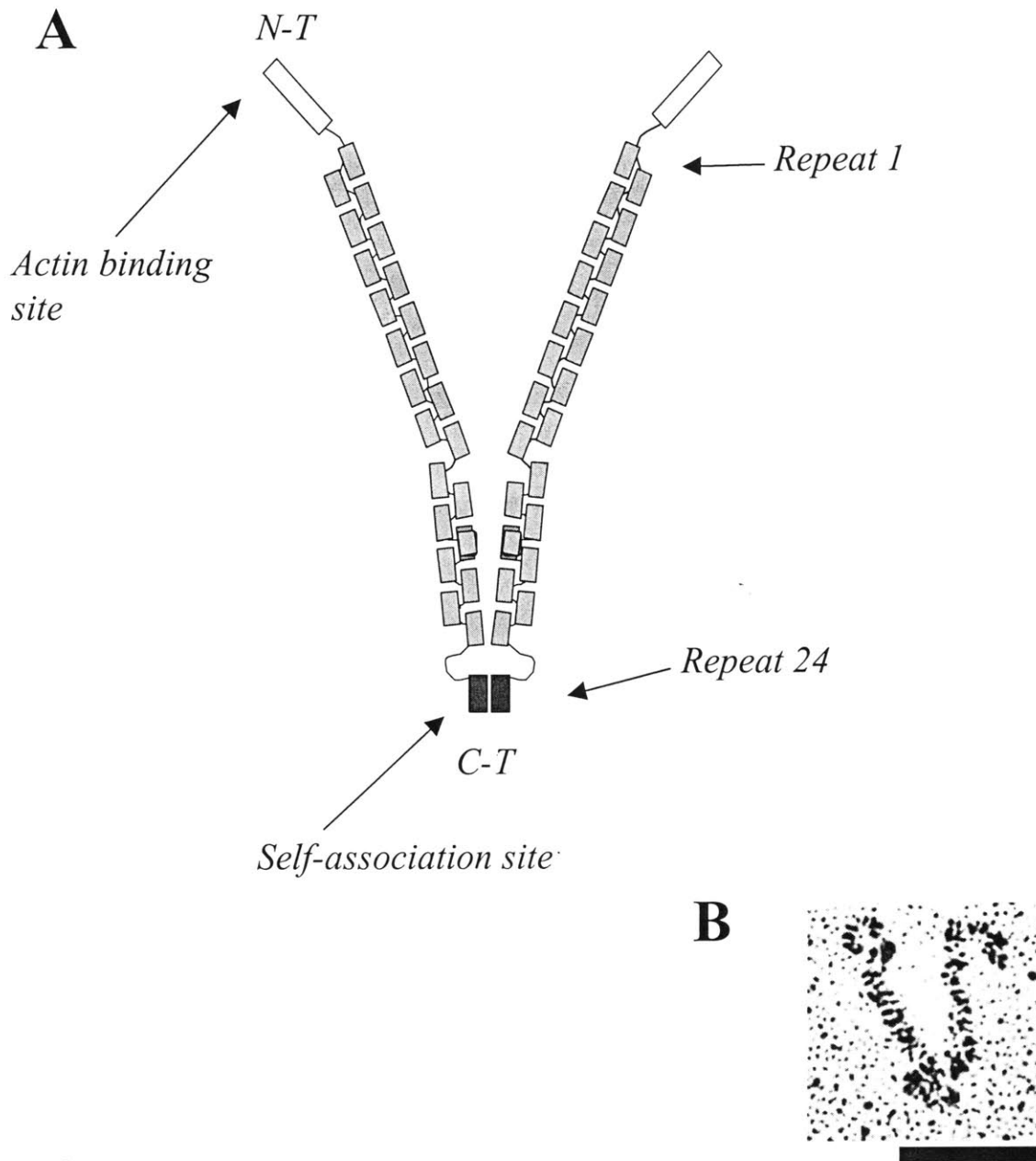
Self-association site

B

Figure 2-1: A. Schematic representation of filamin 1. Note the homodimer morphology. Each arm has the ability to attach to an actin filament at its N terminus, generating a crosslink. B. An electron micrograph of a filamin 1 molecule. Bar 50 nm.

The primary structure of filamin 1 was mapped out by Gorlin et al. [14]. Each subunit is composed of 2647 amino acids (aa). Figure 2-1 shows that the N-terminus (or "head") contains an actin binding domain (274 aa), and the C-terminus (or "tail", 130 aa) contains the self-association site (65 aa) where the two filamin 1 monomers attach to each other to form a dimer. Beyond the actin binding domain the amino acids are grouped into 24 repeat regions along the molecule. Each repeat has approximately 96 amino acids and 7-8 β-sheets folded into an IgG-like motif [10].

There are two irregularities in the primary sequence of each subunit, located between repeats 15/16 and between repeats 23/24. The current theory of filamin 1's structure speculates that these insertions serve as some sort of hinge between the two rigid rod-like domains of a single filamin 1 molecule [14].

2.1.2 Function

Because filamin 1 is a homodimer with its actin binding sites on the ends of two long arms, it is clear that the molecule is well designed to bind two actin filaments together. This efficiency is reinforced by the fact that filamin 1 effectively crosslinks actin filaments into a gel at concentrations near the theoretical minimum. Filamin 1's gel point is 10^{-8} M per 20 μM actin, i.e., one molecule of filamin per 2000 molecules of actin is sufficient to promote gelation! The stoichiometry of filamin in the cell is one molecule per ten subunits of actin.

Since actin plays such a major role in strengthening and stabilizing the cell one would expect actin to be organized into an efficient structure for this purpose and in the presence of filamin 1, actin filaments intersect orthogonally in solution [19]! In the absence of filamin 1, there is no angular preference for the junction of two actin filaments. However, when filamin 1 is added, there is an overwhelming preference for this angle between the two actin filaments to stay at 90°, as can be seen in the electron micrographs in Figure 2-2.

Any model that is developed must agree with both filamin 1's structure as well as its function. The model must accord with the fact filamin 1 is a dimer with known physical dimensions, as well as be able to explain why actin binds orthogonally in the presence of filamin 1.
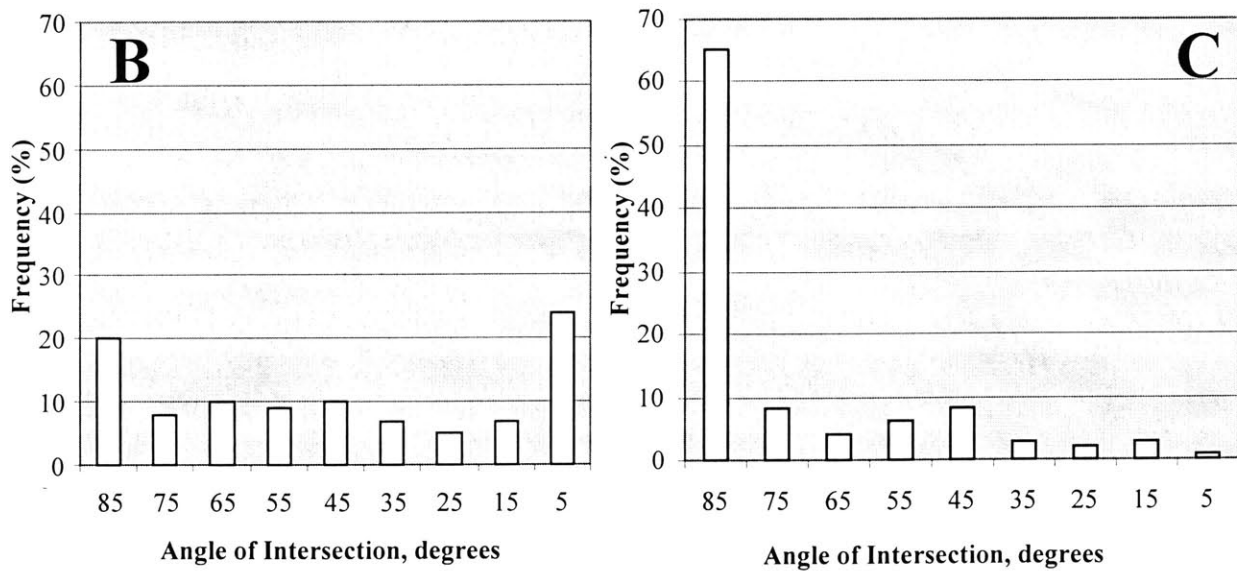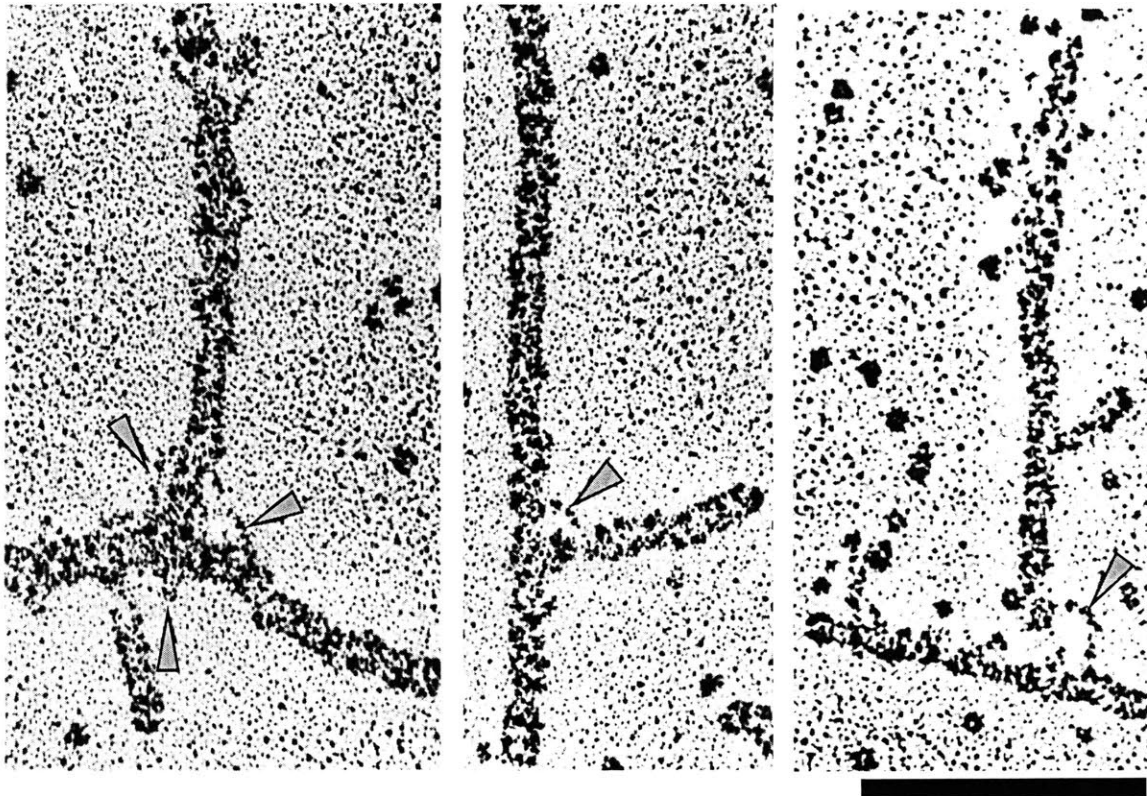
Figure 2-2: A. Orthogonal junctions are visible in these electron micrographs of actin filaments polymerized in the presence of filamin 1. Arrows represent possible filamin 1 molecules localizing near the orthogonal junctions. Bar 100 nm. B. and C. Statistical analysis of the junction angle of actin with and without filamin 1, respectively, as reported by Hartwig [19].

2.2   Viable Models

2.2.1   Tether

The simplest model for filamin 1 binding two actin filaments together is a simple tether. The two actin-binding sites of filamin 1 attach themselves to actin filaments, and hold the filaments together. Filamin 1 would serve as nothing more than a distance constraint, keeping the filaments no more than 160 nm apart. Unfortunately, if filamin 1 is a simple structureless tether, like a shoestring, then there is no way for it to impart orthogonality to the actin filaments.

2.2.2   Electrostatic Repulsion

A more complicated model would allow the filamin 1 to be a flexible tether, but propose another, exterior, mechanism to impart orthogonality.

Since actin filaments are similarly charged particles, when two come in proximity to each other, simple electrostatics explain that they will repel each other. However, if two similarly charged rods are near each other and they are constrained from separating (e.g., by a tether), then they will rotate to a position of force equilibrium (or energy minimization), which will be 90° separation (in the case of symmetry, which is easily justifiable).

However, electrostatics work a little bit differently in ionic solution. In the presence of a large charged molecule, counterions in solution are going to be attracted to the molecule while similarly charged ions will be repelled. The ionic buffer itself then will establish an oppositely charged field, and at sufficient distance, the two fields negate [55]. This negation distance is known as the *DeBye length*. In a buffer similar to physiological cell solution (*in vivo* or *in vitro*), the Debye length of an actin filament is on the order of 1 nm (see Appendix A for equations and calculations).

Because actin filaments are greater than a single nanometer in separation, the electrostatic repulsion model is insufficient to explain the orthogonal binding junctions.

2.2.3   Brace

The simplest model that can support orthogonality is a simple mechanical brace. In this model, the filamin 1 molecule has a consistent structure of some sort, and imparts this structure to actin filaments by binding to them. Presumably, to explain orthogonality, this

structure would involve the filamin 1 subunits having a perpendicular orientation so that when actin filaments bind to them, the actin filaments align in a perpendicular fashion.

2.3 Preliminary Data

In looking at filamin 1 molecules isolated from actin filaments, a consistent shape is seen, a shape that differs from the present understanding of the shape of filamin 1. Figure 2-3 shows several filamin 1 molecules sprayed onto a piece of mica.

Notice first that each filamin 1 molecule seems to have a rigid base region. The self-association site in each molecule is roughly U-shaped. Because this shape seems reproducible in each molecule examined, it implies that this base region where the two C termini attach to each other maintains a high degree of rigidity.

However, this consistent rigidity seems to end approximately 25 nm away from the self-association site (at the approximate location of the "hinge"). Gorlin and Hartwig speculated that the arms of filamin 1 are "rigid rod-like domains" [14]. However, these micrographs indicate that the arms of filamin 1 are highly flexible. Note that there seems to be a high degree of bending and curvature, and that there seems to be no preferred angle of orientation between the arms themselves (as distinguished from the base).

2.4 The Proposed Brace Model

Based on this evidence, we propose a new model for the filamin 1 molecule. This model is divided into two parts: the mechanical structure of the molecule itself, and the mechanism via which the molecule binds to F-actin.

2.4.1 Structure

A filamin 1 molecule can be decomposed into two regions: a stiff base and flexible arms. As a first step, we lay out here the design of experiments to determine the physical properties of the stiff base and the flexible arms, as well as the analysis of these experiments.

The stiff base is what imparts orthogonality to the actin junction. Two actin filaments are joined by a filamin 1 molecule and because the molecule itself contains a nearly orthogonal angle, this large angle is passed on to the filaments. The length of the base region can be determined exactly from electron microscope, but rough observation indicates that the
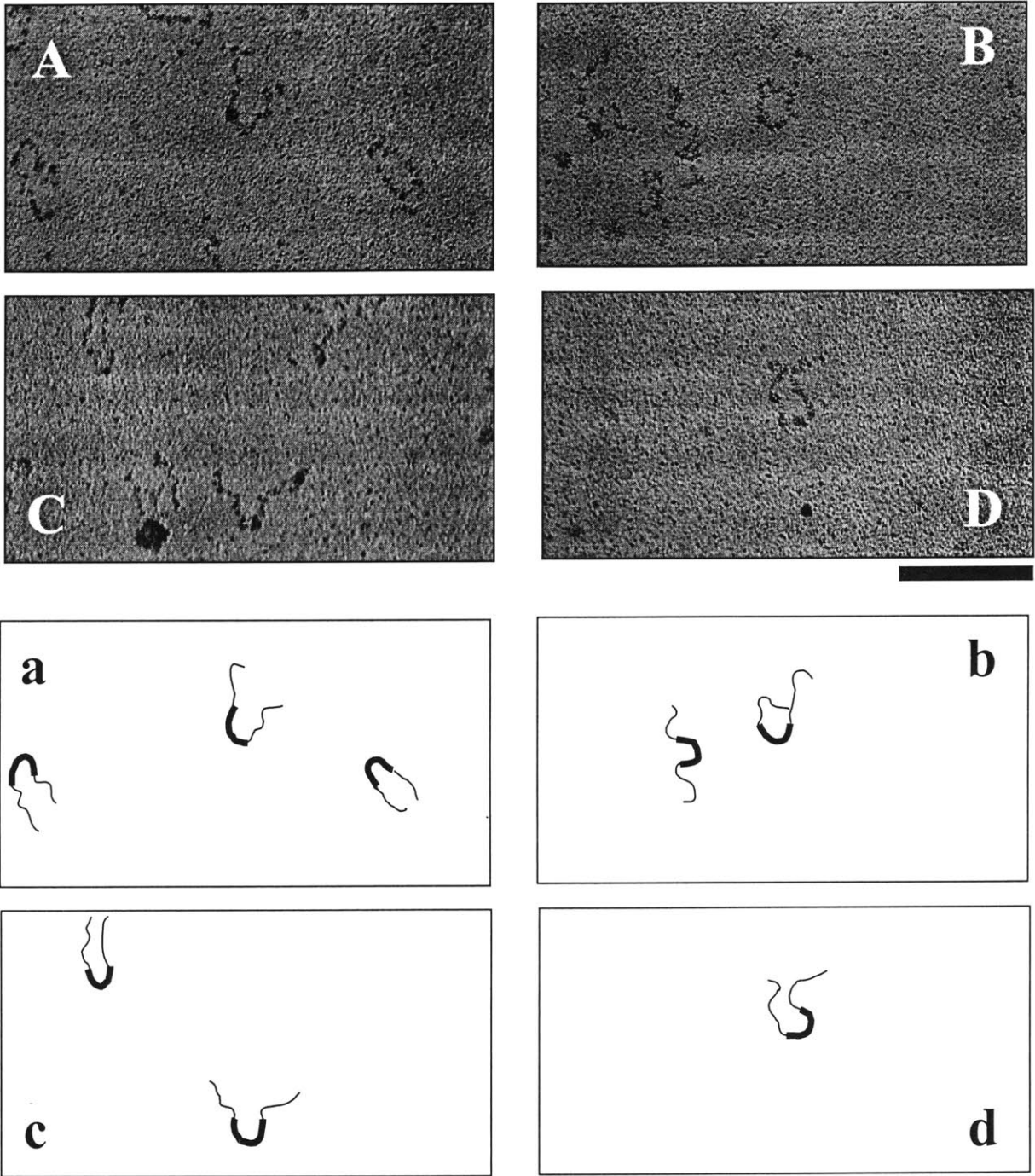
Figure 2-3: A. B. C. D. Electron micrographs of filamin 1. Observe a similar shape in each complete molecule, as shown in schematics a. b. c. d. respectively. There is a consistent U-shaped region in each molecule, and the arms of each are highly curved. Neither of these results has been reported before. Bar 100 nm.

base extends approximately 50 nm along each monomer. Clearly the most important two parameters of the stiff U-shaped base region to be determined experimentally then, are

- the angle subtended by the U-shaped base region, and

- the stiffness of the U-shaped base region, (i.e. k, its resistance to deformation).

The flexible arms are what enable the filamin 1 molecule to attach to actin filaments. Because they essentially serve like flypaper, waving about in solution until they capture an actin filament, their length and flexibility are well-suited to their purpose. The key parameter of the arms to be determined experimentally then, is

- the bending stiffness (EI) of each arm

The design and analysis of this experiment has been performed (Section 3.3.3) and thus this information can be gathered quickly.

2.4.2 Mechanism

The mechanism by which filamin 1 binds to actin filaments is also critical to the validity of this model. Recall that in addition to matching the known structural properties of filamin 1, the key test of the model is its ability to explain orthogonal junctions. While an orthogonal base region by itself seems to allow for orthogonal junctions, there is one key flaw: if the arms are flexible, and the actin binds at the known binding sites at their ends, then there is no way for the shape of the base to influence the actin angle. No matter how rigid and how shaped, if the actin filaments are separated from the base by totally flexible arms, then the actin filaments have no angular constraint.

Thus we propose that the actin filaments must bind *along* the arms of the filamin 1 molecule, all the way to the stiff U-shaped base, as seen in Figure 2-5. This differs from the current hypothesis that actin only binds at the very heads of the arms. This is very important fundamental difference between this model and previous ones. We contend that if the arms are as flexible as they appear, a single binding site at the end of the arms is insufficient to explain orthogonality. The key parameters of the binding mechanism to be determined experimentally then, are

- the angle subtended by two actin filaments when crosslinked
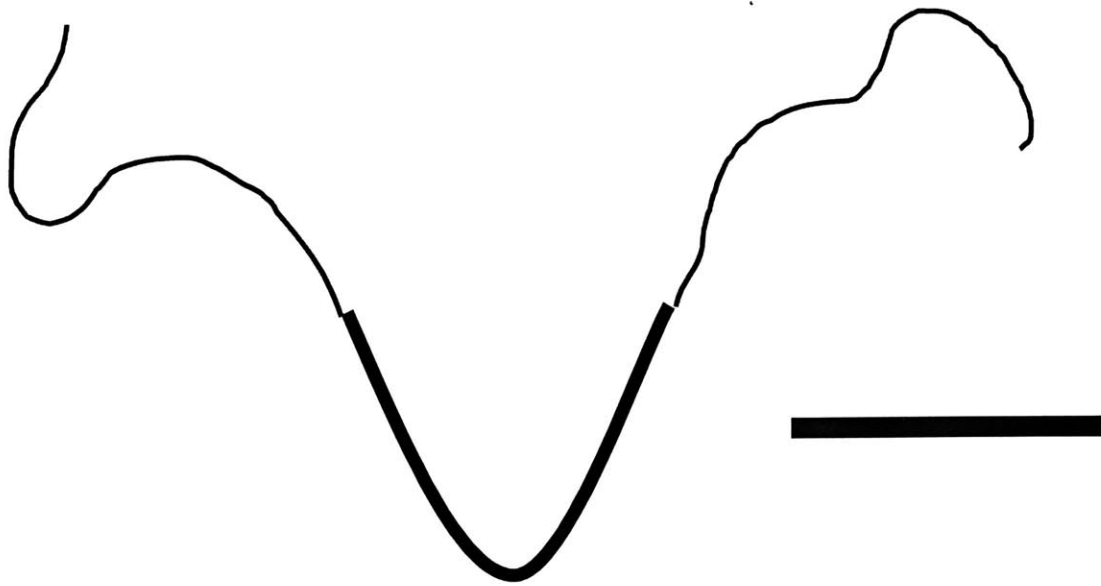
Figure 2-4: Due to such evidence as seen in Figure 2-3, we propose a new model for filamin 1. The base is a stiff region that imparts orthogonality. It is approximately 60 nm long. The arms are highly flexible regions, each about 50 nm long. Bar 30 nm.
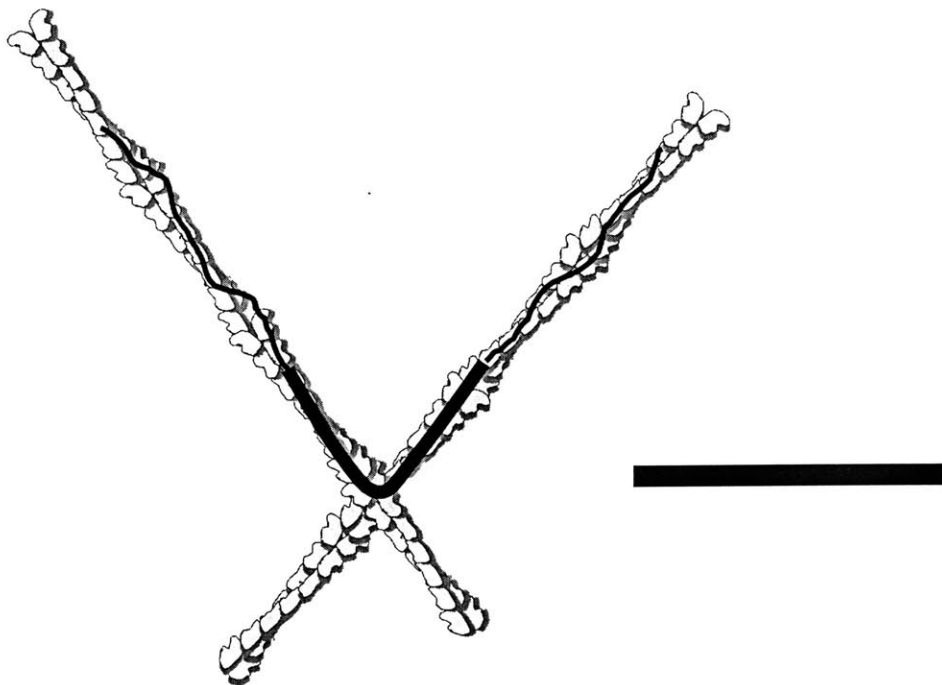
Figure 2-5: The flexible arms of filamin 1 enable the primary binding regions to ensnare actin filaments, like flypaper. Once the initial attachment is made, the arms completely attach along the filaments until the filaments actually attach to the stiff base. At this point, the base is able to impart its angle to the filaments. Bar 50 nm.

- the length of each arm attached to actin

The design and analysis of this experiment has been performed, and thus this information, too, can be gathered quickly. Recall that the motivating question for the model is this: how can the filamin 1 model, as previously proposed, impart orthogonality to the F-actin junction? It appears that it can't. The facts that must be considered are these:

1. Electron micrographs show that the arms of filamin 1 are clearly flexible

2. Actin filaments overwhelmingly bind orthogonally with filamin 1

Hence we propose the Brace Model that incorporates both of these facts into a viable functional predictive model.

Chapter 3

Experimental Method

In Chapter 2 we were able to lay out the model of filamin 1 that we now propose, and also to explain what components of the model need to be studied in order to quantify it. We now explain in detail what experiments we will perform to achieve this goal. First, in Section 3.1 we elaborate on the background preparation necessary for the experiments. In Section 3.2 we explain the scientific procedures that we follow when manipulating the proteins, and the methods we implement to measure the data. Finally, in Section 3.3 we design the actual experiments we will perform in order to gather the requisite data. With each experiment we analyze the mathematical theory involved that will enable us to glean filamin 1's properties from the results.

3.1 Proteins

Filamin 1 is purified from human (uterus) leiomyomas, using methods described previously [17, 52]. The tissue is homogenized in a high salt (1.2 M KI) buffer and then passed through a gel filtration column. Samples from the fractions are run through an SDS 5% acrylamide gel against a high molecular weight marker and platelet lysate. The fractions containing filamin 1 are pooled. These fractions are dialyzed against a low salt (0.1 M KCl) buffer, and then run through an ionic distillation column with a gradient buffer between 0.1 M and 0.4 M KCl. Again the fractions are run though an SDS 5% acrylamide gel and the fractions containing filamin 1 are pooled. In order to increase the concentration of filamin 1, the filamin 1 is dialyzed against glycerol (removing the water), and then dialyzed against 0.3 M KCl buffer (increasing the concentration by a factor of 4). This filamin 1 solution

is then checked for potency with a falling ball viscosity/cross-linking assay, and the final concentration of the filamin 1 is determined using spectrophotometry.

Actin is isolated from the leg and back muscles of rabbits by the procedure of Spudich and Watt [46] except that 0.8 M KCl is substituted for 0.6 M KCl during the first polymerization cycle. G-actin is passed through a sterile 0.45 μm Millipore filter and stored at 4°C in 0.5 mM ATP, 0.5 mM 2-mercaptoethanol, 0.2 mM $CaCl_2$, 2 mM Tris·HCl (pH 8.0). G-actin is polymerized to F-actin by adding KCl to a final concentration of 0.1M and incubating at 20°C for 1 h.

3.2 Procedures

3.2.1 Electron Microscopy

The morphology of filamin 1 and the structures formed by the mixtures of actin with filamin 1 are studied in a Philips 301 electron microscope, using rotary shadowing at low angles or freeze-etching.

Rotary Shadowing

For rotary shadowing, the technique of Tyler and Branton [50] is used. A total of 0.18 ml of F-actin (0.56 mg/ml) in 0.1M KCl, 0.05mM ATP, 0.05mM 2-mercaptoethanol, 0.02mM $CaCl_2$, 0.2mM Tris·HCl (pH 7.5) is mixed with 0.02 ml of filamin 1 (1 mg/ml) in 0.1M KCl, 10mM imidazole·HCl (pH 7.5) and incubated for 5 min at room temperature. The protein solution is diluted with 9 vol. 48% (v/v) glycerol and sprayed onto mica. The mica is dried under vacuum at room temperature and rotary shadowed with platinum/carbon on an uncooled rotary specimen stage of a Balzers freeze-etch apparatus. This is done using Balzers electron bombardment guns and a quartz crystal film thickness monitor as described by Tyler and Branton [50]. A 4.5° shadow angle is employed, giving a heavy metal deposition of 0.7 to 0.8 nm. The replicas are examined in a Philips 301 electron microscope at 80 kV.

Freeze Etching

The protein sample is prepared as before. 3 μl are placed on a coverslip and slammed onto a gold table half-submersed in liquid helium. The frozen sample is then etched and dried

under vacuum at -100°C. After drying the sample is rotary shadowed with platinum/carbon on a cooled rotary specimen stage of a Balzers freeze-etch apparatus using Balzers electron bombardment guns and a quartz crystal film thickness monitor as described by Tyler and Branton [50]. A 4.5° shadow angle is employed, giving a heavy metal deposition of 0.7 to 0.8 nm. The replicas are examined in a Philips 301 electron microscope at 80 kV.

3.2.2 Data Collection and Analysis

Negative stereo pair images are taken of the protein molecules magnified 25,000 times. These films are developed by hand and then enlarged another six times and reversed with an Ilford Multigrade 500 enlarger, and then printed as 8.5"x11" prints with an Ilford 2150 RC direct photo paper printer. These images, or sections thereof, are digitized using a Minolta 3CCD reflex digital camera, with a resolution of 1600 x 1200 pixels. The resulting digital images are then analyzed using a computer imaging program designed by Yuan Cheng for this purpose: reconstructing stereo pairs of filament images into the original three dimensional structure. This output is then inputted into a computer imaging program designed by Celine Paloc which is able to view this three dimensional network from any angle, and calculate steric relations between any two points. The combination of the EM and the two computer software packages enables one to measure distances and other physical properties from electron microscopy samples.

3.3 Experimental Design

3.3.1 Angle of U-shaped Base Region

In order to determine the angle of the actin junction and how the presence of filamin 1 affects this angle, it is important to understand the shape of filamin 1 itself. Hence we examine filamin 1 molecules in order to characterize their shape. The most important shape property of the Brace Model is the angle of the stiff base region.

Filamin 1 is prepared for electron microscopy and freeze-etched as described above, and observed via pictures taken by electron microscopy. With a large sample size, the angle of the U-shaped base region of each molecule is measured. The process is somewhat iterative. Based on observation, the length of the flexible arms is determined to be roughly 50 nm. For each molecule then, three points are chosen: two points 50 nm away from the ends of

the molecules (the ends of the U-shaped base region), and a point 80 nm from each end (the midpoint of the U-shaped base region), as in Figure 3-1. Using the midpoint as the vertex, the angle of the intersection of these line segments is measured as the angle of the U-shaped base region.

3.3.2 Stiffness of U-shaped Base Region

Theory

Due to the small size of the filamin 1 molecule, controlled forces cannot be applied to it. Rather, the forces must be observed passively as the molecule is acted upon by the thermal agitation of the buffer surrounding it. Random Brownian forces dominate the kinetics of a molecule of the size dealt with here. Since the filamin 1 molecule is small and since its arms have little resistance to bending, the best way to apply forces directly to the filamin 1 molecule is via large actin filaments. Actin filaments are attached to the ends of the filamin 1 for two reasons. First, their greater size allows for greater forces to be applied, and larger forces mean larger (and easier to measure) deformations. Second, using rigid rods simplifies the analysis, rather than attempting to determine the kinetics of moving flexible arms. Third, there may be an interaction between the actin and the filamin 1 that modifies the filamin 1, and we would like to determine the stiffness of the filamin 1 when it is crosslinking actin. Lastly, the actin filaments are able to be fluorescently labeled, and thus the experiments can be repeated using fluorescent microscopy as a check.

We model the U-shaped base region as a damped driven harmonic oscillator with unknown stiffness, as seen in Figure 3-2. The filamin 1 molecule is driven by random Brownian interactions with the molecules of the solution. The filamin 1 molecule is damped by the same molecules of solution, which give rise to drag.

Obviously the forces applied are functions of time, and so the deformation is a function of time. Because the carbon replica of the sample produced for electron microscopy (a snapshot in time) does not contain any explicit information about the forces being imparted, there is no way to directly correlate the force and deformation at a given instant in time. We would like to discover a method to determine the stiffness of the system merely by observation of the position of the system over time. The solution of this problem involves writing the
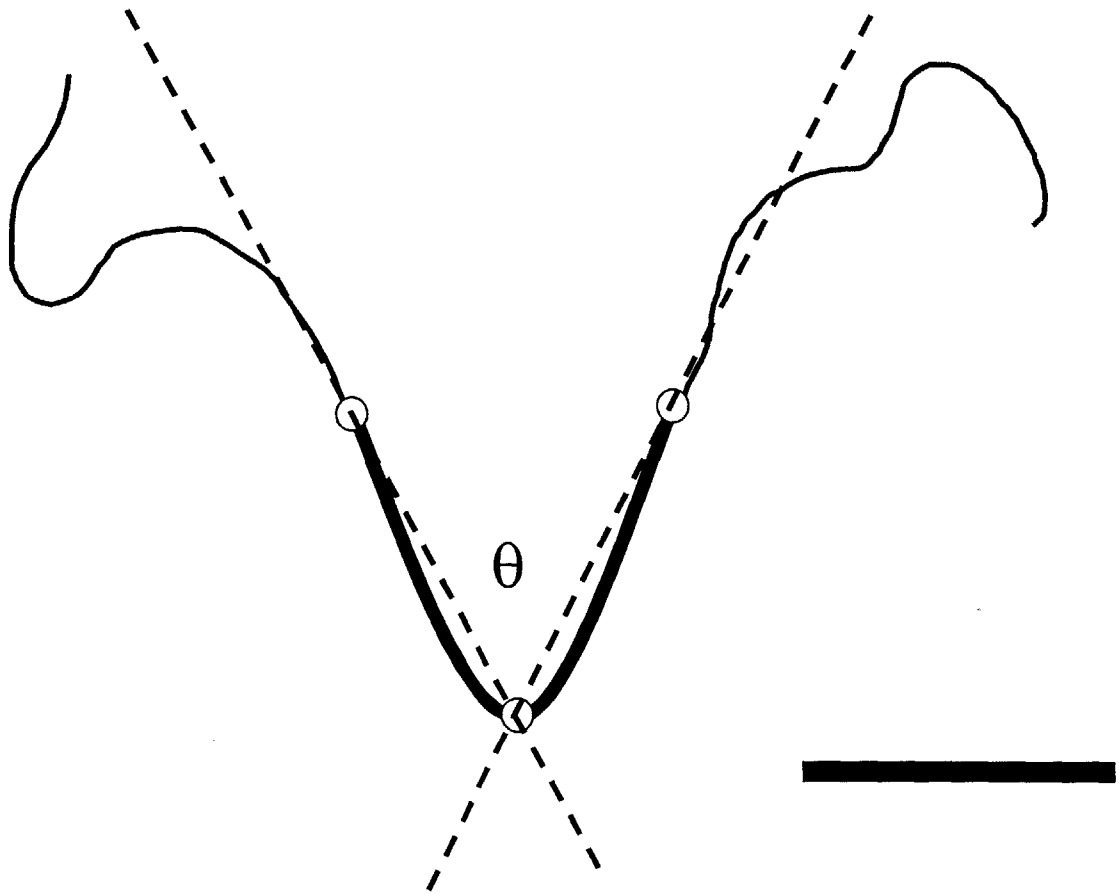
Figure 3-1: Measurement of the angle of the U-shaped base region of filamin 1. Bar 30 nm.

equation of motion for the system, starting from the first principle

$$\sum T = I\alpha \tag{3.1}$$

where $\sum T$ is the sum of all external torques on the system, I is the moment of inertia of the system being studied, and α is the angular acceleration of the system.

All scientists studying Brownian motion, from Einstein [6] to Doi [5], have made certain fundamental assumptions. The forces due to the environment are broken into two components: a frictional drag term and a random force due to molecular collisions. Therefore the equation of motion can be revised to include these specific terms, as well as the spring force.

$$-\beta I\dot{\theta} + IA(t) - k_T\theta = I\ddot{\theta} \tag{3.2}$$

where $-\beta I$ is the drag coefficient, $IA(t)$ is a random torque due to the surrounding medium, k_T is the resistance to deformation due to the spring (filamin 1), and I is the moment of inertia of the rigid rod (actin).

The first term on the LHS is the frictional drag term and is a property of the shape of the object and the properties of the fluid medium. Although random in nature, several things are assumed about the fluctuating component and have been assumed here as elsewhere. First, $A(t)$ is assumed to be a Gaussian process with mean zero. Second, $A(t)$ has an infinitely short correlation time [5, 41, 51]. The first assumption is reasonable if the object is much larger than the impinging molecules, since that means many collisions must occur in order to produce motion, and in that event the central limit theorem applies. The second assumption is also reasonable since the molecular time scale of collisions is far smaller than the time scale of the object's motion [41]. Note that both of the fluid terms result from the motion of the molecules of the fluid in which the object is placed. The same molecules that impinge on the object to move it also produce friction to resist motion of the object. One cannot isolate the two physically, although we do mathematically.

Following Kittel [28], who follows Langevin, and ultimately Einstein [6], we proceed to solve the problem by premultiplying Equation 3.2 by θ/I, yielding

$$-\beta\theta\dot{\theta} + \theta A(t) - \frac{k_T\theta^2}{I} = \theta\ddot{\theta} \tag{3.3}$$
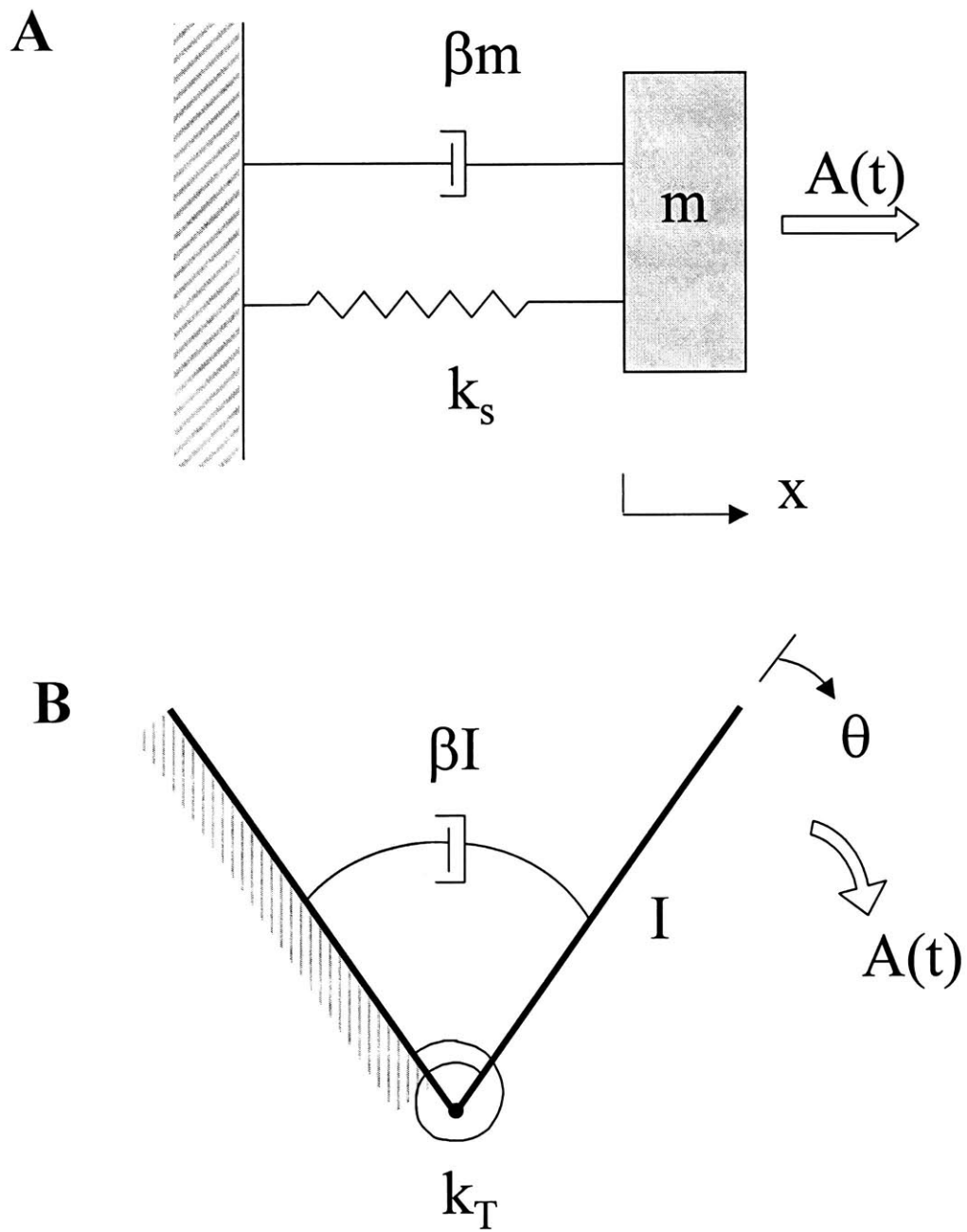
Figure 3-2: Modeling the actin-filamin 1 system as a damped driven harmonic oscillator. A. The standard linear DDHO. B. The analogous angular DDHO.

Writing the nonlinear cross terms as derivatives, we now have

$$-\frac{\beta}{2}\frac{d}{dt}(\theta^2) + \theta A(t) - \frac{k_T \theta^2}{I} = \frac{1}{2}\frac{d^2}{dt^2}(\theta^2) - \dot{\theta}^2 \tag{3.4}$$

Because the system is intuitively ergodic, rather than look at one system and measure its position over time, we can instead look at many systems at any time and perform the same statistical analysis. Ergodicity ensures that the many systems in the ensemble "act" as snapshots of one system in time. If we now take the ensemble average looking at many identical systems (and factor out the constants) we have

$$-\frac{\beta}{2}\left\langle \frac{d}{dt}(\theta^2) \right\rangle + \langle \theta A(t) \rangle - \frac{k_T}{I}\left\langle \theta^2 \right\rangle = \frac{1}{2}\left\langle \frac{d^2}{dt^2}(\theta^2) \right\rangle - \left\langle \dot{\theta}^2 \right\rangle \tag{3.5}$$

According to our assumptions above, the random term $A(t)$ averages out to 0. Also, the last term on the RHS can be rewritten according to the equipartition theorem $\frac{1}{2}I\left\langle \dot{\theta}^2 \right\rangle = \frac{1}{2}k_B T$, leaving

$$-\frac{\beta}{2}\left\langle \frac{d}{dt}(\theta^2) \right\rangle - \frac{k_T}{I}\left\langle \theta^2 \right\rangle = \frac{1}{2}\left\langle \frac{d^2}{dt^2}(\theta^2) \right\rangle - \frac{k_B T}{I} \tag{3.6}$$

Fortunately time derivatives and ensemble averages can be exchanged because differentiation is a linear operator, as shown here:

$$\frac{d}{dt}\langle \theta(t) \rangle = \frac{d}{dt}\left(\frac{1}{N}\sum_{k=1}^{N} \theta^{(k)}(t) \right) = \frac{1}{N}\sum_{k=1}^{N}\frac{d\theta^{(k)}}{dt} = \left\langle \frac{d\theta(t)}{dt} \right\rangle \tag{3.7}$$

When we do this Equation 3.6 becomes

$$-\frac{\beta}{2}\frac{d}{dt}\left\langle \theta^2 \right\rangle - \frac{k_T}{I}\left\langle \theta^2 \right\rangle = \frac{1}{2}\frac{d^2}{dt^2}\left\langle \theta^2 \right\rangle - \frac{k_B T}{I} \tag{3.8}$$

which we can rewrite as

$$\frac{d^2}{dt^2}\left\langle \theta^2 \right\rangle + \beta\frac{d}{dt}\left\langle \theta^2 \right\rangle + \frac{2k_T}{I}\left\langle \theta^2 \right\rangle = \frac{2k_B T}{I} \tag{3.9}$$

This is just a second order linear differential equation in $\left\langle \theta^2 \right\rangle$ which yields the steady state solution for the variance of position,

$$\left\langle \theta^2 \right\rangle = \frac{k_B T}{k_T} \tag{3.10}$$

31

Boltzmann's constant, k_B, is 1.380662×10^{-23} J/K. So at a room temperature of 295 K, to be used in our experiments, we have the relationship

$$k_T \left\langle \theta^2 \right\rangle = 4.07 \times 10^{-23} J \tag{3.11}$$

This equation relates the torsional stiffness of filamin 1, k_T, to the variance of the angle between crosslinked actin filaments. The units of k_T are N · m (a force resistance to angular deformation has the same units as energy).

Technique

Actin is polymerized in the presence of gelsolin and filamin 1. Gelsolin is a known severing and capping protein that regulates F-actin length. Placing it in solution with actin with a molar ratio of 1:50 produces short filaments approximately 200 nm long, well below the 15 μm persistence length of actin [24] (defined precisely in the following section, 3.3.3), such that these short filaments can be considered stiff rods (again discussed in Section 3.3.3).

The filamin 1-actin samples are prepared for electron microscopy as described above. Data consists of pictures taken from the electron microscope. Using the same technique as described above and illustrated in Figure 3-1, the angle of each filamin 1 molecule is measured, and statistics are compiled. The mean and variance of the angular distribution are calculated.

The mean yields an important piece of information: the inherent angle of a filamin 1 molecule that is crosslinking two actin filaments. The variance can be put into Equation 3.11, producing a numerical value for k_T. This value is the stiffness of filamin 1 that we seek.

3.3.3   Flexibility of Flexible Arm Region

Theory

The standard metric for stiffness when dealing with polymer dynamics is the "persistence length." Qualitatively speaking the persistence length is the maximum length over which bending is negligible (i.e. if $L < L_p$, the filament can be modeled as a rigid rod). If we examine the tangential angle of a curve measured relative to some axis, shown as $\theta(s)$ in Figure 3-3, then the persistence length is the length above which the angle $\theta(s)$ becomes

uncorrelated in three dimensions. Quantitatively, the persistence length is defined as

$$L_p = \frac{EI}{k_B T} \tag{3.12}$$

Numerically, the persistence length can be determined by relating the bending energy of a filament to its thermal energy. From solid mechanics we know the bending energy, $U(s)$, of a beam is related to the curvature $\frac{d\theta}{ds}(s)$ according to

$$U = \frac{1}{2} EI \int\limits_0^L \left(\frac{d\theta}{ds} \right)^2 ds \tag{3.13}$$

Computer tracing algorithms can calculate $\theta(s)$ at any point on an image of a filament. We can resolve the trace of the filament into independent cosine modes using Fourier analysis [12, 24]. The equipartition theorem of physics ensures that each independent energy mode contributes $\frac{1}{2} k_B T$ to the total energy [43].

Since we are using a computer to analyze images, the data is inherently discrete, not continuous (Figure 3-3 B). If we write the Fourier decomposition of modes discretely as

$$\theta(s) = \sqrt{\frac{2}{L}} \sum_{n=0}^{\infty} a_n \cos \left(\frac{n\pi s}{L} \right) \tag{3.14}$$

then we can write the bending energy as

$$U = \frac{1}{2} EI \sum_{n=1}^{\infty} \frac{n\pi}{L} (a_n)^2 \tag{3.15}$$

Each quadratic term in Equation 3.15, because it represents an independent energy mode, contributes $\frac{1}{2} k_B T$ to the total energy. Hence

$$\mathrm{var}\, \langle a_n \rangle = \frac{k_B T}{EI} \times \left(\frac{L}{n\pi} \right)^2 \tag{3.16}$$

Finally then,

$$L_p = \frac{EI}{k_B T} = \frac{L^2}{n^2 \pi^2 \mathrm{var}\, \langle a_n \rangle} \tag{3.17}$$

A

$\theta(s)$

s

B

Δs_1 Δs_2 Δs_3 θ_5

k=1

k=2 k=3
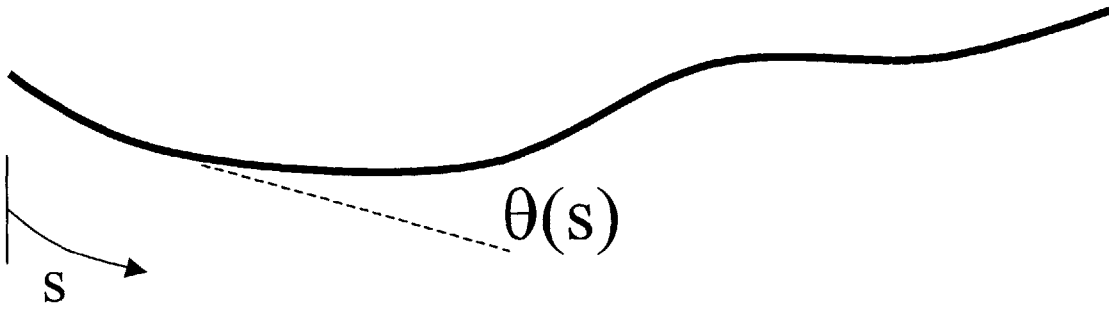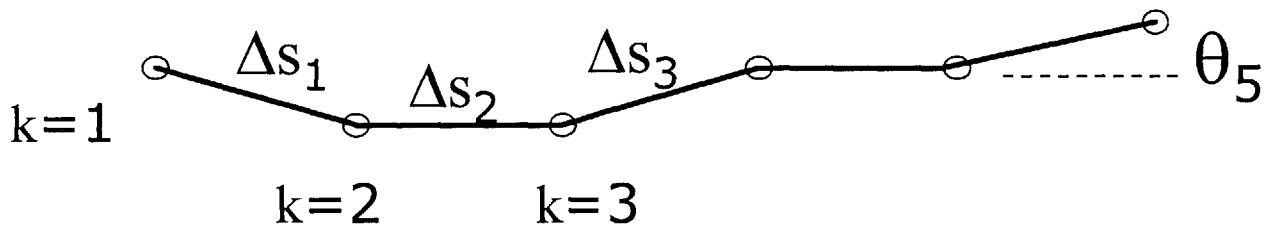
Figure 3-3: Calculating the persistence length of filamin 1's flexible arms. A. A two-dimensional continuous trace of an arm of filamin 1. B. A discretized representation of the same arm.

Technique

Filamin 1 is prepared for electron microscopy as described above. Data consists of photographs taken from the electron microscope. For each of the flexible arms of each filamin 1 molecule, a trace is produced using the software of Cheng and Paloc (see Section 3.2.2), and then resolved into Fourier modes using MATLAB. The variance of the amplitude of each mode (first, second, third,...nth) over many samples can be computed, var $\langle a_n \rangle$, and Equation 3.17 can be solved for L_p.

3.3.4 Length of Filamin 1-Actin Attachment

The filamin 1-actin samples are prepared for electron microscopy as described above. Data consists of photographs taken from the electron microscope. A representative micrograph is shown in Figure 3-4. For each filamin 1-actin complex, the length of each arm overlapping the actin filament is measured, and statistics are compiled.
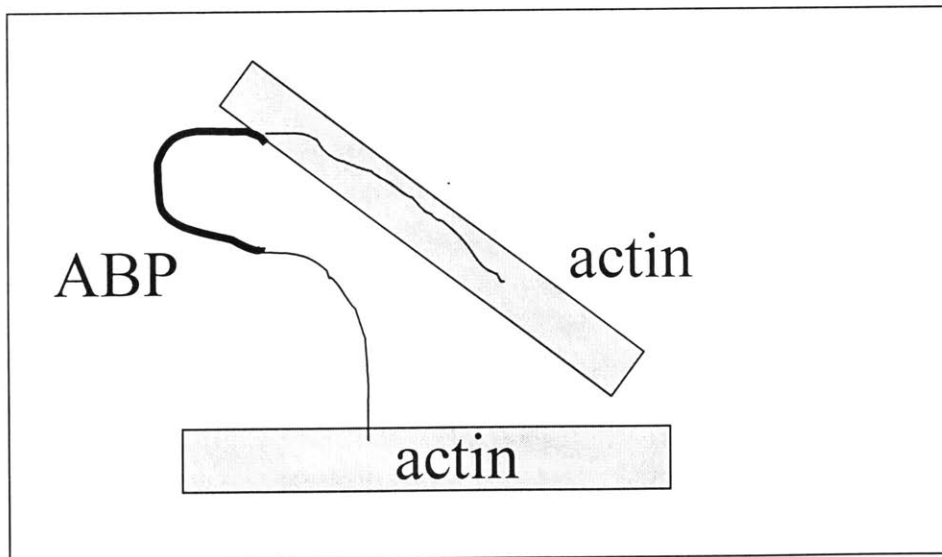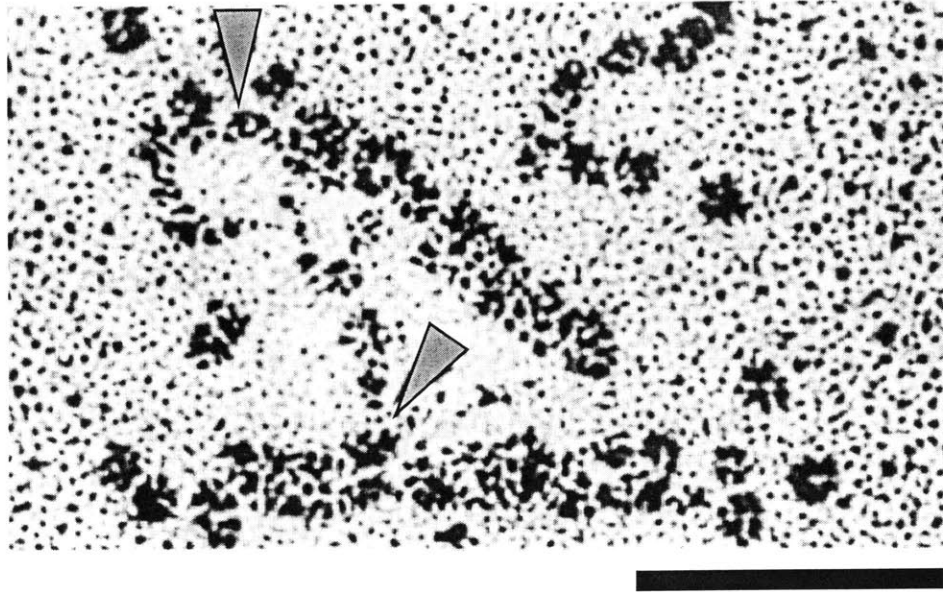
Figure 3-4: A representative micrograph showing filamin 1-actin attachment length. Note the arrows indicate two interesting attachment mechanisms: the top arrow is where filamin 1 is binding along the filament and the bottom arrow is where filamin 1 is binding at one point on the filament. Bar 50 nm.

Chapter 4

Discussion

Several future experiments immediately present themselves to verify the results we will gather with the experiments explained here.

The previous model for filamin 1 has only two actin binding sites. We have shown that only two actin binding sites, along with flexible arms, are not able to produce orthogonal junctions. We would like to show directly, for the first time, that filamin 1 has more than just two actin binding sites. A more direct protein assay could be used to remove the known actin binding sites from the filamin 1 molecule's N terminus to validate the conclusion that the entire length of the arms serve as actin binding sites. If these new "decapitated" filamin 1 molecules still attach to actin, and more importantly still promote orthogonal junctions, then the modified proteins must still contain actin binding sites.

Another future experiment could use an entirely different technique to verify the stiffness data. The experiments we lay out here use electron microscopy since that is a high-resolution technique that enables us to see many junctions and analyze them simply. Another technique we could use to gather this same data would be fluorescent microscopy. Electron microscopy has the advantage of being very high resolution (on the order of nanometers) and generating data simply. In a micrograph, the molecules are stuck to glass and coated with metal. Everything is motionless and visible. But electron microscopy has disadvantages too. Sample preparation disturbs the system. First the molecules are rapidly frozen as they are dropped onto a hard surface. Then they are thawed and coated with hot metal. Perhaps the dynamics of this system are not the same as the protein system *in vitro*. Perhaps this treatment alters angular orientations. This is where light microscopy has its advantages.

Actin and filamin 1 are both far too small to be seen directly under a light microscope, but this problem is easily circumvented by attaching fluorophores to the proteins. Fluorophores can be excited with laser light, which triggers them to emit visible light. Unfortunately the light emitted by the fluorophore is 100 times broader than the proteins themselves. We have circumvented this problem also by writing an intensity tracing program to plot the actual actin location from data gathered from pixel intensity. Fortunately the emitted light distribution, known as the *Airy distribution*, is of a known form. So we wrote a MATLAB macro that takes advantage of this distribution. Operating on a digital image captured by NIH Image software, the program proceeds along the length of the filament, measuring the intensity values of the pixels across the filament (each pixel is on the order of 100 nm). At each location, it produces an intensity curve. Using least squares analysis, the program fits a curve to the intensity data, and generates the location the actual filament must be in in order to emit this particular Airy distribution. The program then connects the centers along the filament in order to trace the filament. This method enables us to not only improve on the natural resolution limit of light microscopy, but it also enables us to resolve location more precisely the dimension of a single pixel. It only requires the user to demarcate the two ends of a filament. So fluorescent microscopy enables us to watch the actin-filamin 1 system moving around in real time. Unfortunately, even with all these ingenious fixes, fluorescent microscopy still has some disadvantages; namely, binding fluorophores to proteins modifies the proteins' physical properties. Fortunately we are interested in learning about filamin 1, so if we add fluorophores (like rhodamine phalloidin) to actin, we have only made it more rigid, and the rigidity of actin is one of our assumptions. A more serious drawback of fluorescent microscopy is the difficulty in gathering data. One must prevent the actin from binding to glass in order to watch the motion of the system. But when the system moves around in three dimensions, analyzing a two-dimensional picture becomes problematic. It is difficult to determine the "true" angle between the filaments from the 2-D projection. We are developing a way to constrain the system's translation. It appears that electron microscopy and fluorescent microscopy are two complementary ways to gather the information we need.

Another modification we can make in order to strengthen our results is to label the filamin 1 fluorescently. In both microscopy techniques, there is some uncertainty as to whether or not a given junction is regulated by filamin 1. With electron microscopy, there

is no way of telling if a junction is even a junction or merely two filaments laying on top of each other (fluorescent microscopy allows us to see if the two filaments are moving together in time). By adding a fluorophore to filamin 1 molecules (which has never been done), we could determine immediately if two actin filaments are crosslinked by filamin 1. In fluorescent microscopy, this immediately enables us to discard random intersections not regulated by filamin 1. Unfortunately, as with actin mentioned above, binding a fluorophore to the filamin 1 physically modifies the filamin 1, and thus corrupts the data. Hence the best method would be to determine the binding efficiency of filamin 1 using a fluorophore, and then apply that information when interpretting non-labeled systems.

We now have the first model based on experiment that explains how filamin 1 and F-actin interact. The future goal of this project, after gathering the data, will be to extrapolate this data to increasingly complicated structures of actin and filamin 1, as well as determining how this protein interaction affects cell motility and actin turnover.

Chapter 5

Conclusions

Reviewing known information for filamin 1 and actin, a new model has been suggested for the filamin 1 molecule. Contrary to previous views, the model is broken down into several regions. There is a stiff U-shaped base that imparts orthogonality to F-actin junctions, and has a large natural angle. Attached to the base are two highly flexible arms. The expected low value of the stiffness indicates that they have no resistance to bending, and very beautifully explains how filamin 1 molecules attract filaments. Once captured, actin filaments bind the full length of the flexible arms, indicating that they bind all the way to the stiff base.

In order to quantify the model, several experiments have been created and carefully designed, and are ready to be performed. Analysis of the results has already taken place, and thus as soon as the data is recorded, the results will be known. The primary parameters to be determined are

- the natural angle of the stiff base, both with and without actin attached

- the stiffness of the base

- the flexibility of the arms

- the length of each arm attached to actin

The natural angle of the stiff base will be determined by direct observation of molecules with electron microscopy. The stiffness of the base will be calculated by examining many actin-filamin 1 junctions, measuring the variance of the angle of the junction, and relating

the two according to Equation 3.10. The flexibility of the arms will be determined by analyzing the curvature of the arms according to Section 3.3.3. The length of each arm that attaches to the actin filaments will be observed from direct electron micrographs of the system.

We now have the first model based on experiment that explains how filamin 1 and F-actin interact. The future goal of this project, after gathering the data, will be to extrapolate this data to increasingly complicated structures of actin and filamin 1, and ultimately construct a predictive model of the entire actin cytoskeleton.

Appendix A

Debye Length Calculation

This explanation is modeled after Weiss [55]. The results can be seen in Figure A-1.

Poisson's equation is derivable from Gauss's law, and relates the charge density, ρ, to the electric potential, ψ. In one dimension, Poisson's equation is

$$\frac{d^2(\psi(x))}{dx^2} = -\frac{\rho}{\varepsilon} \tag{A.1}$$

Naturally the total charge is just the sum total of each type of charge present, so that

$$\rho(x) = z^+ F c^+ - z^- F c^- \tag{A.2}$$

The concentration, c, of each ion will establish itself as an exponential decay in a state of equilibrium, satisfying the Nernst-Planck equation such that the flux of the nth ion is zero. If we assume that $c^+(\infty) = c^-(\infty) = C$ and that $z^+ = z^- = z$, then

$$c^+(x) = C e^{-\frac{zF\psi(x)}{RT}} \tag{A.3}$$

$$c^-(x) = C e^{\frac{zF\psi(x)}{RT}} \tag{A.4}$$

where z is the valence of the ion in solution, F is a physical constant known as Faraday's constant, and RT is the thermal energy per mole.

When equations A.1 -- A.4 are solved simultaneously for $\psi(x)$, the result is that
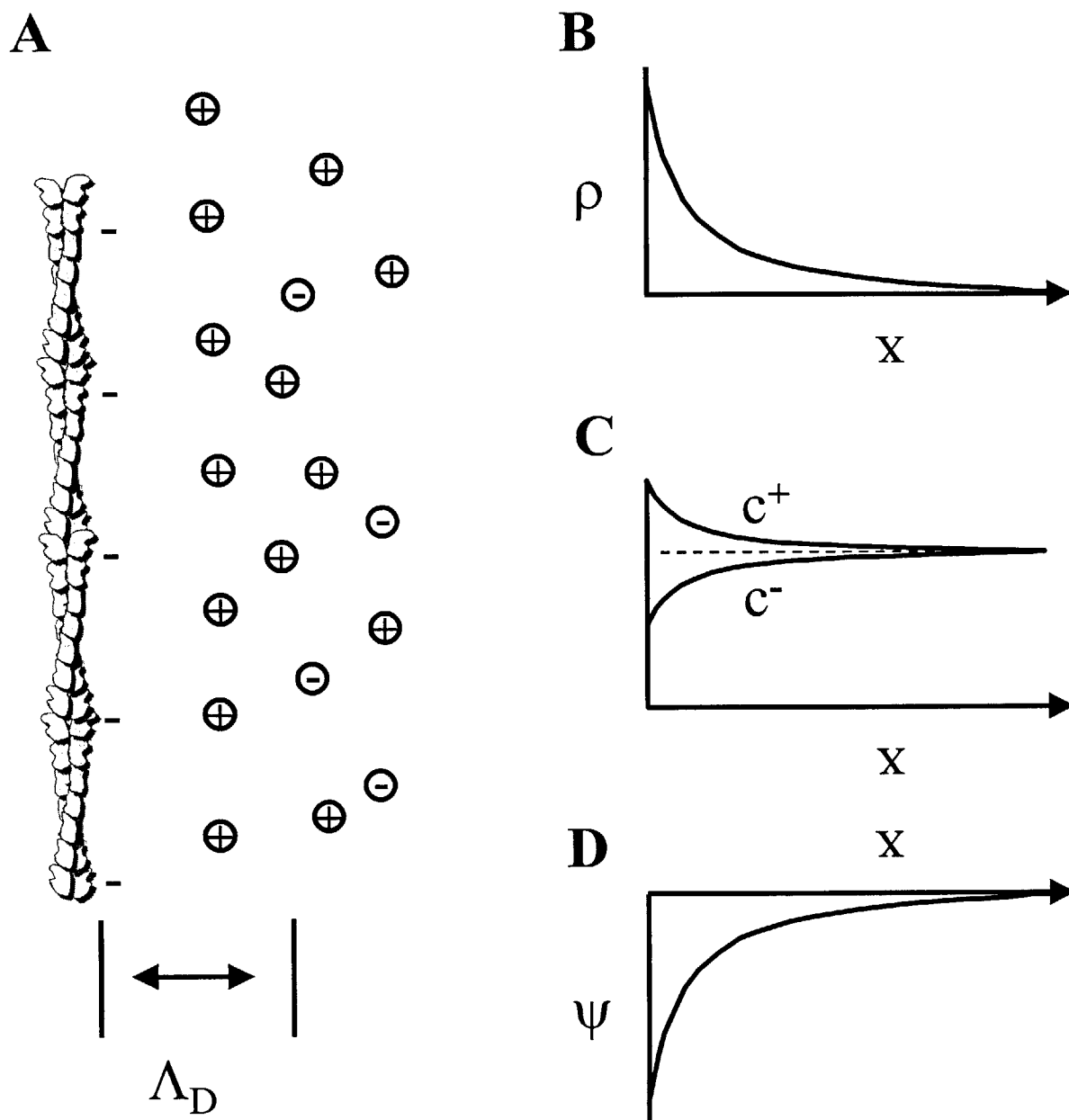
$$\psi(x) = e^{\frac{x}{\Lambda_D}} \tag{A.5}$$

42

Figure A-1: A. Pictorial representation of the ions distancing themselves from the charged body. B. C. and D. The exponential drop off of charge density, concentration, and potential field, respectively, with distance.

where

$$\Lambda_D = \sqrt{\frac{\varepsilon RT}{2z^2 F^2 C}} \qquad (A.6)$$

is the length scale of the exponential decay of the electric field.

Now, $F = 9.65 \times 10^4$ C/mol, $R = 8.314$ J/Kmol, $T = 300$ K, and $\varepsilon = 7.08 \times 10^{-10}$F/m, so the Debye length varies with C and z.

We can look at various ions in the cell to determine the order of Λ_D. For Mg^{++} ($z = 2$), the physiological concentration is $C = 6$ mM [55] so the Debye length, $\Lambda_{D,Mg}$, is 2 nm. Similarly $[Cl^-]= 75$ mM, so $\Lambda_{D,Cl}$ is 0.5 nm; $[Na^+]= 20$ mM, so $\Lambda_{D,Na}$ is 2 nm; $[K^+]= 150$ mM, so $\Lambda_{D,K}$ is 1 nm.

Bibliography

[1] S. Burlacu, P. A. Janmey, and J. Borejdo. Distribution of actin filament lengths measured by fluorescent microscopy. *American Journal of Physiology*, pages C569–C577, 1992.

[2] H. Cantiello, A. Prat, J. Bonventre, C. Cunningham, J. Hartwig, and D. Ausiello. Actin-binding protein contributes to cell volume regulatory ion channel activation in melanoma cells. *Journal of Biological Chemistry*, 286:4596–4599, 1993.

[3] C. Cunningham. Actin polymerization and intracellular solvent flow in cell blebbing. *Journal of Cell Biology*, 129:1589–1599, 1995.

[4] C. Cunningham, J. Gorlin, D. Kwiatkowski, J. Hartwig, P. Janmey, H. Byers, and T. Stossel. Actin binding requirement for cortical stability and efficient locomotion. *Science*, 255:325–327, 1992.

[5] Masao Doi and Sam F. Edwards. *The Theory of Polymer Dynamics*. Oxford Science Publications, 1986.

[6] Albert Einstein. *The Theory of Brownian Motion*. Dover, 1926.

[7] Jan Faix, Michael Steinmetz, Heike Boves, Richard Kammerer, Friedrich Lottspeich, Ursula Mintert, John Murphy, Alexander Stock, Ueli Aebi, and Gunther Gerisch. Cortexillins, major determinants of cell shape and size, are actin-bundling proteins with a parallel coiled-coil tail. *Cell*, 86:631–642, 1996.

[8] G. Forgacs. On the possible role of cytoskeletal filamentous networks in intracellular signaling: an approach based on percolation. *Journal of Cell Science*, 108:2131–2143, 1995.

[9] J. Fox, E. Lamperti, Y. Eksioglu, S. Hong, I. Scheffer, W. Dobyns, B. Hirsch, R. Radtke, S. Berkovic, P. Huttenlocher, and C. Walsh. Mutations in filamin I arrest migration of cerebral cortical neurons in human periventricular heterotopia. *Neuron*, 21:1315–1325, 1998.

[10] P. Fucini, C. Renner, C. Herberhold, A. Noegel, and T. Holak. The repeating segments of the F-actin cross-linking gelation factor ABP-120 have an immunoglobulin-like fold. *Nature Structural Biology*, 4:223–230, 1997.

[11] Lorna Gibson and Bob Ashby. *Cellular Solids: Structure and Properties*. Pergamon, 1988.

[12] Frederick Gittes, Brian Mickey, Jilda Nettleton, and Jonathon Howard. Flexural rigidity of microtubules and actin filaments measured from thermal fluctuations in shape. *Journal of Cell Biology*, 120:923–934, 1993.

[13] J. Gorlin, E. Henske, S. Warren, C. Kunst, M. D'Urso G. Palmieri, J. Hartwig, G. Bruns, and D. Kwiatkowski. Actin-binding protein (ABP-280) filamin gene (FLN) maps telomeric to the color vision locus (R/CGP) and centromeric to G6PD in Xq28. *Genomics*, 17:496–498, 1993.

[14] Jed B. Gorlin, Rina Yamin, Sheila Egan, Murray Stewart, Thomas P. Stossel, and John H. Hartwig. Human endothelial actin-binding protein (ABP-280, nonmuscle filamin): A molecular leaf spring. *Journal of Cell Biology*, 111:1089–1105, 1990.

[15] Enrico Grazi, Giorgio Trombetta, Ermes Magri, Paolo Cuneo, and Christine Schwienbacher. α Actinin from chicken gizzard: At low temperature, the onset of actin gelling activity correlates with actin bundling. *Biochemical Journal*, 298:129–133, 1994.

[16] John H. Hartwig and Patty Shelvin. The architecture of actin filaments and the ultrastructural location of actin-binding protein in the periphery of lung macrophages. *Journal of Cell Biology*, 103:1007–1020, 1986.

[17] John H. Hartwig and Thomas P. Stossel. Cytochalasin B and the structure of actin gels. *Journal of Molecular Biology*, 134:539–553, 1979.

[18] John H. Hartwig and Thomas P. Stossel. Structure of macrophage actin-binding protein molecules in solution and interacting with actin filaments. *Journal of Molecular Biology*, 145:563–581, 1981.

[19] John H. Hartwig, Jonathon Tyler, and Thomas P. Stossel. Actin binding protein promotes the bipolar and perpendicular branching of actin filaments. *Journal of Cell Biology*, 87:841–848, 1980.

[20] Donald Ingber. The architecture of life. *Scientific American*, 278:48–57, 1998.

[21] Herve Isambert, Pascal Venier, Anthony C. Magg, Abdelatif Fattoum, Ridha Kassab, Dominique Pantaloni, and Marie-France Carlier. Flexibility of actin filaments derived from thermal fluctuations. *Journal of Biological Chemistry*, 270:11437–11444, 1995.

[22] Paul A. Janmey, Soren Hvidt, George F. Oster, Jennifer Lamb, Thomas P. Stossel, and John H. Hartwig. Effect of ATP on actin filament stiffness. *Nature*, 347:95–99, 1990.

[23] George G. Judge. *The Theory and Practice of Econometrics*. John Wiley and Sons, 1985.

[24] Joseph Kas, H. Strey, M. Barmann, and E. Sackmann. Direct measurement of the wave-vector-dependent bending stiffness of freely flickering actin filaments. *Europhysics Letters*, 21:865–870, 1993.

[25] Joseph Kas, H. Strey, and E. Sackmann. Direct imaging of reptation for semiflexible actin filaments. *Nature*, 368:226–229, 1994.

[26] Joseph Kas, H. Strey, J. X. Tang, D. Finger, R. Ezzell, E. Sackmann, and P. A. Janmey. F-actin, a model polymer for semiflexible chains in dilute, semidilute, and liquid crystalline solutions. *Biophysical Journal*, 70:609–625, 1996.

[27] Akiyoshi Kishino and Toshio Yanagida. Force measurements by micromanipulation of a single actin filament by glass needles. *Nature*, 334:74–76, 1988.

[28] Charles Kittel. *Elementary Statistical Physics*. Wiley, 1958.

[29] E. Maestrini, C. Patrosso, M. Mancini, S. Rivella, , M. Rocchi, M. Repetto, A. VIlla, A. Frattini, M. Zoppe, P. Vezzoni, and D. Toniolo. Mapping of two genes encoding

isoforms of the actin-binding protein ABP-280, a dystrophin like protein, to Xq28 and to chromosome 7. *Human Molecular Genetics*, 2:761–766, 1993.

[30] Paul Matsudaira. Mapping structural and functional domains in actin-binding proteins.

[31] Paul Matsudaira. Modular organization of actin crosslinking proteins. *Trends in Biochemical Sciences*, 16:87–92, 1991.

[32] Paul Matsudaira. Actin crosslinking proteins at the leading edge. *Cell Biology*, 5:165–174, 1994.

[33] Paul Matsudaira and Paul Janmey. Pieces in the actin severing puzzle. *Cell*, 54:139–140, 1988.

[34] James McConnell. *Rotational Brownian Motion and Dielectrics*. Academic Press, 1980.

[35] James L. McGrath, Y. Tardy, C. F. Dewey Jr., Y. Kuang, and J. H. Hartwig. Actin dynamics correlate with cell motility in an endothelial wound healing model. Prepublished.

[36] Alexander Mogilner and George Oster. Cell motility driven by actin polymerization. *Biophysical Journal*, 71:3030–3045, 1996.

[37] Edward Nelson. *Dynamical Theories of Brownian Motion*. Princeton University Press, 1967.

[38] R. Niederman, P. C. Amrein, and J. H. Hartwig. Three-dimensional structure of actin filamants and of an actin gel made with actin-binding protein. *Journal of Cell Biology*, 96:1400–1413, 1983.

[39] Ralph Nossal. On the elasticity of cytoskeletal networks. *Biophysical Journal*, 53:349–359, 1988.

[40] Yasutaka Ohta, Nobuchika Suzuki, John Hartiwg, and Shun Nakamura. Actin-Binding Protein-280 (ABP-280) is a downstream effector for the RalA GTPase which regulates filopodia formation. Prepublished.

[41] W. E. Parry, R. E. Turner, D. ter Haar, J. S. Rowlinson, G. V. Chester, N. M. Hugenholtz, and R. Kubo. *Many Body Problems*. W. A. Benjamin, 1969.

[42] D. Pocopio, S. da Silvo, C. Cunningham, and R. Mortara. *Trypanosoma cruzi*: Effect of protein kinase inhibitors and cytoskeletal protein organization and expression on host cell invasion by amastigotes and metacyclic trypomastigotes. *Experimental Parasitology*, 90:1–13, 1998.

[43] F. Reif. *Fundamentals of Statistical and Thermal Physics*. McGraw-Hill, 1965.

[44] Robert L. Satcher and C. Forbes Dewey Jr. Theoretical estimates of mechanical properties of the endothelial cell cytoskeleton. *Biophysical Journal*, 71:109–118, 1996.

[45] Raymond A. Serway. *Physics for Scientists and Engineers*. Saunders College Publishing, 1983.

[46] J. A. Spudich and S. Watt. The regulation of rabbit skeletal muscle contraction 1. Biochemical studies of the interaction of the tropomyosin-troponin complex with actin and the proteolytic fragments of myosin. *Journal of Biological Chemistry*, 246:4866–4871, 1971.

[47] Thomas P. Stossel, John. H. Hartwig, John Condeelis, Angelika A. Noegel, Michael Schleicher, and Sandor S. Shapiro. The filamins: Integrators of structures and signals at the cytoplasm-membrane interface. Prepublished.

[48] Julie A. Theriot and Timothy J. Mitchison. Actin microfilament dynamics in locomoting cells. *Nature*, 352:126–131, 1991.

[49] Yuri Tsuda, Hironori Yasutake, Akihiko Ishjima, and Toshio Yanagida. Torsional rigidity of single actin filaments and actin-actin bond breaking force under torsion measured directly by *in vitro* micromanipulation. *Proceedings of the National Academy of Sciences*, 93:12937–12942, 1996.

[50] Jonathan Tyler and D. Branton. Rotary shadowing of extended molecules dried from glycerol. *Journal of Ultrastructural Resolution*, 71:95–102, 1980.

[51] G. E. Uhlenbeck and L. S. Ornstein. On the theory of Brownian motion. *Physical Review*, 36:823–841, 1930.

[52] K. Wang. Filamin, a new high-molecular-weight protein found in smooth muscle and nonmuscle cells. Purification and properties of chicken gizzard filamin. *Biochemistry*, 16:1857–1865, 1977.

[53] Y. L. Wang. Exchange of actin subunits at the leading edge of living fibroblasts: Possible role of treadmilling. *Journal of Cell Biology*, 101:597–602, 1985.

[54] A. Wegner. Head to tail polymerization of actin. *Journal of Molecular Biology*, 108:139–150, 1976.

[55] Thomas Fischer Weiss. *Cellular Biophysics: Transport.* MIT Press, 1996.

[56] Jan Wilhelm and Erwin Frey. Radial distribution function of semiflexible polymers. *Physics Review Letters*, 77:2581–2584, 1996.

[57] Jingyuan Xu, Denis Wirtz, and Thomas D. Pollard. Dynamic cross-linking by α-actinin determines the mechanical properties of actin filament networks. *Journal of Biological Chemistry*, 273:9570–9576, 1998.

Biography

Christopher Allan Hartemink was born at 3:18 a.m. on October 22, 1974 in Falls Church, Virginia to two Dutch immigrants. He started his promising academic career at the age of four at Kent Gardens Elementary School. He remembers recess and show-and-tell the most vividly. In 1980 the family Hartemink moved to Fort Myers, Florida so Chris attended Tanglewood Elementary School for grades 1–5. Ceramics and cursive, as well as a smattering of introductory algebra kept Chris excited there. He then attended Fort Myers Middle School for grades 6–8. Amazingly inspiring teachers like Mr. Wilkinson and Mrs. Cannady honed Chris's nascent love for learning into a passion. Chris attended Fort Myers High School for grades 8–12. FMHS was a very challenging public school due to its strong AP program and gifted teachers like Mr. Gault and Mrs. Marderness (it was recently ranked one of the top fifty high schools in the country). In the fall of 1992 Chris chose to continue his academic marathon at Calvin College. Knowing that college is what you make of it, and also that he would end up in grad school, Chris passed up big-name expensive institutions in favor of a liberal arts education, caring professors in small classes, and an opportunity to grow. Over his four years at Calvin, Chris studied engineering, physics, math, and philosophy, picking up a couple majors and a minor. More importantly, he developed relationships that will last him for life. Chris is now a graduate student in the HST division of the Massachusetts Institute of Technology and Harvard Medical School. He hopes to finish someday.

In his free time, Chris enjoys all manners of sports (from ultimate to mountain biking to soccer to waterskiing), and especially reading. He dabbles in chess and crossword puzzles, has an iguana, worships the Simpsons, thinks John Calvin is the bomb, and loves Sam.